HHS Public Access

Author manuscript

J Magn Reson Imaging. Author manuscript; available in PMC 2020 December 01.

Published in final edited form as:

J Magn Reson Imaging. 2019 December ; 50(6): 1798–1807. doi:10.1002/jmri.26781.

Ungated Nonenhanced Radial Quiescent Interval Slice-Selective (QISS) Magnetic Resonance Angiography of the Neck: Evaluation of Image Quality

Ioannis Koktzoglou, Ph.D.[1,2], **Emily A. Aherne, M.B. B.Ch.**[1,3], **Matthew T. Walker, M.D.**[1,2], **Joel R. Meyer, M.D.**[1,2], **Robert R. Edelman, M.D.**[1,3]

[1]Department of Radiology, NorthShore University HealthSystem, Evanston, USA

[2]University of Chicago Pritzker School of Medicine, Chicago, USA

[3]Northwestern University Feinberg School of Medicine, Chicago, USA

Abstract

Background: Standard-of-care time-of-flight (TOF) techniques for nonenhanced magnetic resonance angiography (NEMRA) of the carotid bifurcation and other cervical arteries often provide non-diagnostic image quality due to motion and flow artifacts.

Purpose: To perform an initial evaluation of an ungated radial quiescent-interval slice-selective (QISS) technique for NEMRA of the neck, in comparison with 2D TOF and contrast-enhanced magnetic resonance angiography (CEMRA).

Study Type: Retrospective.

Population: 60 patients referred for neck MR angiography.

Field Strength/Sequence: Ungated radial QISS at 3 Tesla.

Assessment: Three radiologists scored image quality of 18 arterial segments using a 4-point scale (1, non-diagnostic; 2, fair; 3, good; 4, excellent), and two radiologists graded proximal internal carotid stenosis using 5 categories (<50%, 50–69%, 70–99%, occlusion, non-diagnostic).

Statistical Tests: Friedman tests with post-hoc Wilcoxon signed-rank tests; unweighted Gwet's AC1 statistic; tests for equality of proportions.

Results: Ungated radial QISS provided image quality that significantly exceeded 2D TOF (mean scores of 2.7 versus 2.0, 2.7 versus 2.2 and 2.9 versus 2.3; $P<0.001$, all comparisons), while CEMRA provided the best image quality (mean scores of 3.6, 3.7, and 3.5 for the three reviewers). Inter-rater agreement of image quality scores was substantial for CEMRA (AC1=0.70, $P<0.001$), and moderate for QISS (AC1=0.43, $P<0.001$) and TOF (AC1=0.41, $P<0.001$). Compared to TOF, QISS NEMRA provided a significantly higher percentage of diagnostic segments for all three reviewers (91.0% versus 71.7%, 93.5% versus 72.9%, 95.5% versus 85.2%; $P<0.0001$) and

To Whom Correspondence Should be Addressed: Ioannis Koktzoglou, Ph.D., Evanston Hospital, Walgreen Jr. Building, Suite G507, 2650 Ridge Ave., Evanston, IL 60201, Tel: (847) 570-4288, Fax: (847) 570-2942, ikoktzoglou@gmail.com.

demonstrated better agreement with CEMRA for grading of proximal internal carotid stenosis (AC1=0.94 versus 0.73 for reviewer 1, $P<0.05$; AC1=0.89 versus 0.68 for reviewer 2, $P<0.05$).

Data Conclusion: In this initial study, ungated radial QISS significantly outperformed 2D TOF for the evaluation of the neck arteries with overall better image quality and more diagnostic arterial segments, and improved agreement with CEMRA for grading stenosis of the proximal internal carotid artery.

Keywords

Magnetic resonance angiography; neck; carotid bifurcation; quiescent-interval slice-selective (QISS); time-of-flight; nonenhanced

INTRODUCTION

Suspected arterial disorders of the carotid bifurcation and other cervical arteries are routinely evaluated using a combination of time-of-flight (TOF) nonenhanced magnetic resonance angiography (NEMRA) and first-pass contrast-enhanced magnetic resonance angiography (CEMRA). Compared with TOF, first-pass CEMRA provides better accuracy, larger anatomical coverage, and shorter scan times (1–5). Nonetheless, TOF techniques remain useful in providing a localizer for placement of the CEMRA imaging volume, for the evaluation of patients in whom contrast administration is contraindicated or undesirable (e.g. those with severe renal insufficiency), and when contrast medium is being reserved for the evaluation of cerebral perfusion using first-pass dynamic imaging techniques (6, 7). TOF also provides a backup to CEMRA in case of technical failure, e.g. due to early or late arrival of the contrast bolus with respect to the center of k-space, or excess patient motion.

Given the well-recognized drawbacks of 2D and 3D TOF (3, 8), several alternative NEMRA techniques have been proposed (9–12). However, these techniques have yet to provide the speed, spatial coverage, and resistance to flow and motion artifacts needed to reliably evaluate the carotid bifurcation and other cervical arteries.

Quiescent interval slice-selective (QISS) is an ECG-gated non-contrast MRA technique with proven accuracy for evaluation of the lower-extremity peripheral arteries (13, 14). However, applying the QISS technique to the neurovascular circulation requires several adaptations. For instance, ECG leads are not typically placed on the patient for head and neck MRA studies. In addition, shimming is less robust in the neck versus lower extremities, resulting in off-resonance artifacts from the balanced steady-state free precession (bSSFP) readout. To address these concerns, ungated versions of the QISS technique that do not require placement of ECG leads were developed and a fast low-angle shot (FLASH) readout that is largely immune to off-resonance artifacts was substituted for the bSSFP readout. In addition, a radial k-space trajectory was found advantageous to minimize motion artifacts from swallowing and respiration. Given promising results in pilot studies (15, 16), an ungated radial QISS FLASH protocol was incorporated into our standard-of-care neck MRA exam on 3 Tesla MRI scanners used for both inpatient and outpatient imaging. The purpose of this retrospective study was to evaluate the performance of this protocol in comparison to standard-of-care 2D TOF and CEMRA.

MATERIALS AND METHODS

Patients

This retrospective study was approved by our institutional review board; the need for informed consent was waived. We retrospectively reviewed neck MRA studies done at 3 Tesla without and with contrast material between November 1, 2017 and May 1, 2018. Study inclusion criteria were age ≥18 years and referral for neck MRA performed with 2D TOF NEMRA, QISS NEMRA, and CEMRA. Study exclusion criteria included the following: lack of scan data for any of the three acquisitions (TOF, QISS, CEMRA) including renal impairment that precluded Gadolinium-based CEMRA (defined by glomerular filtration rate lower than 30mL/min/1.73m^2), previous arterial revascularization including stent placement, and test not conducted to an acceptable standard (e.g. RF leak interference). After excluding 30 studies for the above reasons (see flow diagram in Figure 1), we identified 60 patients who were included in our final analysis.

Imaging System and Protocols

Imaging was performed on 3 Tesla MRI systems (MAGNETOM Skyra and MAGNETOM Skyra Fit, Siemens Healthcare, Erlangen, Germany) providing maximum gradient strengths of 45mT/m and gradient slew rates of 200mT/m/ms, and equipped with 20-channel head and neck coils. Imaging was performed with 2D TOF, 2D QISS, and 3D CEMRA, all without cardiac gating. TOF and CEMRA were acquired using institutional standard-of-care protocols. CEMRA was performed with injection of 0.1mmol/kg of gadobutrol (Gadavist, Bayer HealthCare, Whippany, NJ) into an antecubital vein at 2mL/s. Typical imaging parameters are provided in Table 1.

QISS NEMRA consisted of a 3-shot radial FLASH readout that was preceded by in-plane and tracking superior inversion radiofrequency (RF) pulses for suppression of background and venous signals. No cardiac gating was used. A stack of 128 slices tilted 45° away from the axial plane and centered at the approximate level of the carotid bifurcation was acquired, providing ≈24cm of axial coverage. In comparison with purely axial slices, the use of a tilted acquisition increases axial coverage by approximately 41% without adversely affecting image quality (15). A total of 204 radial k-space views were acquired, and a golden (≈111.25°) angular increment between successively acquired radial k-space views was applied.

Image Analysis

Image processing was performed on a workstation (Leonardo; Siemens Healthcare, Erlangen, Germany) by an MRI scientist (I.K.) who did not participate in image scoring. After non-vascular background tissue was cropped using a 3D volume visualization and editing tool, rotating maximum intensity projection image sets (45 projections separated by 8°) were created from each MR angiographic volume of each patient. These image sets were then anonymized, randomized, placed in a designated study folder in the picture archiving and communications system server, and then independently reviewed by three radiologists (E.A., M.W., J.M.) who were blinded to patient name, clinical history, and results of other diagnostic procedures. One radiologist (reviewer 1) had 6 months of fellowship training in

neuroradiology (E.A.), whereas two radiologists (reviewers 2 and 3) had certificates of added qualification in neuroradiology with >15 years of experience interpreting neurovascular MRA (M.W., J.M.).

Image quality was scored for the following 18 segments: 1 - aortic arch; 2 - brachiocephalic artery; 3 and 4 - bilateral common carotid arteries; 5 and 6 - bilateral proximal internal carotid arteries; 7 and 8 - bilateral cervical segments of the internal carotid arteries; 9 and 10 - bilateral petrous and cavernous segments of the internal carotid arteries; and 11 through 18 - bilateral V1, V2, V3, and V4 segments of the vertebral arteries. The following 4-point scoring system was used: 1 = non-diagnostic, image quality inadequate for diagnosis; 2 = fair, image quality marginally acceptable for diagnosis; 3 = good, image quality adequate for confident diagnosis; and 4 = excellent, excellent image quality providing a highly-confident diagnosis. Partially or not imaged vessel segments as deemed by at least one reviewer were excluded from evaluation. The proportion of arterial segments rated as diagnostic (score of ≥2) by each reviewer was computed. Intra-rater agreement of image quality scoring was done by a secondary review and scoring of 12 (20%) randomly selected patients (36 image sets) at least 3 months after the first scoring session.

Grading of Proximal Internal Carotid Stenosis

Two radiologists (reviewers 1 and 2) independently graded the severity of stenosis at the proximal internal carotid artery using the following grading scale: 1 = normal patency or <50% stenosis; 2 = 50–69% stenosis; 3 = 70–99% stenosis; 4 = occlusion; and 5 = non-diagnostic/indeterminate. All gradings were based on visual interpretation of rotating maximum intensity projection image sets. CEMRA was used as the reference test because it provides high diagnostic accuracy (17, 18), and because X-ray digital subtraction angiography is not routinely performed at our institution due to invasiveness and associated procedural risks. Due to the lack of a reference test, vessels graded as non-diagnostic on CEMRA by each reviewer were excluded from the agreement analysis for that reviewer. Inter-rater agreement of stenosis gradings were computed for QISS, TOF, and CEMRA. Stenosis gradings were also dichotomized into the categories of <50%, and ≥50% stenosis for the calculation of sensitivity and specificity for the detection of ≥50% stenosis; for each of the two reviewers, listwise deletion across the three imaging techniques was applied to handle non-diagnostic/indeterminate gradings.

Statistical Analysis

List-wise deletion was used to handle missing image quality scores which occurred if an arterial segment was outside the imaged field of view. Differences in image quality scores were identified using Friedman tests and post-hoc Wilcoxon signed-rank tests. Unweighted Gwet's AC1 statistic (19) was used to determine inter-rater and intra-rater agreement of image quality scores, as well as inter-sequence and inter-rater agreement in the grading of proximal internal carotid artery stenosis; agreement was interpreted as follows: 0.01–0.20, slight; 0.21–0.40, fair; 0.41–0.60, moderate; 0.61–0.80, substantial; and 0.81–0.99, almost perfect (20). Mean image quality (computed across all arterial segments and reviewers) was correlated with age and body mass index using the Spearman rank correlation coefficient (ρ). Differences in proportions were assessed using tests for equality of proportions.

Bonferroni corrected *P*-values less than 0.05 indicated statistical significance. Analyses were done using R software (The R Foundation for Statistical Computing, Vienna, Austria).

RESULTS

Patient Demographics

Sixty adult patients (26 men, 34 women; mean age, 61.7±17.1 years, mean body mass index, 26.5±4.9) who underwent TOF, QISS and CEMRA in the same scan session were included in this study. Indications for imaging included weakness (n=10), headache (n=8), visual field disturbance (n=7), suspected stroke (n=6), dysphasia (n=5), numbness (n=5), dizziness (n=3), vertigo (n=2), altered mental status (n=2), transient ischemic attack (n=1), syncope (n=1), suspected carotid artery dissection (n=1), suspected vertebral artery dissection (n=1), pulsatile tinnitus (n=1), infarct (n=1), hypertension and cardiac arrest (n=1), Horner syndrome (n=1), coronary artery dissection and non-ST-elevation myocardial infarction (n=1), convulsion (n=1), carotid stenosis (n=1), and aneurysm (n=1).

Image Quality

A total of 1080 arterial segments (60 subjects, 18 segments per subject) were evaluated for potential scoring. Excluding arterial segments that were outside the field of view and unscorable by at least one reviewer (4 of 1080 for CEMRA, 112 of 1080 for QISS, and 117 of 1080 for TOF), a total of 908 segments that were portrayed by all three techniques and scored by all three reviewers were included for further analysis. These 908 segments were interpreted by three reviewers, resulting in a total of 2724 evaluations.

Representative angiograms obtained with ungated radial QISS are shown in Figure 2, Figure 3, Figure 4, and Figure 5. The proportions of arterial segments deemed diagnostic by the three reviewers for each protocol are listed in Table 2. The proportion of diagnostic arterial segments displayed by QISS approached that provided by CEMRA, and for all three reviewers, significantly surpassed the proportion of diagnostic segments provided by TOF ($P<0.0001$). Non-diagnostic image quality scores for QISS were due to signal saturation artifact (see Figure 3) as well as to respiratory artifact primarily in the aorta and proximal arterial segments.

Image quality scores for each technique and arterial segment are summarized in Table 3. When scores were averaged across all eighteen arterial segments, CEMRA provided the best image quality, with mean scores of 3.6, 3.7, and 3.5 for reviewers 1, 2, and 3 ($P<0.001$), followed by QISS (mean scores of 2.7, 2.7, and 2.9 for reviewers 1, 2, and 3) which provided the second highest image quality scores, and TOF (mean scores of 2.0, 2.2, and 2.3 for reviewers 1, 2, and 3) which provided the lowest image quality scores. QISS provided better image quality than TOF in 15 of 18, 13 of 18, and 15 of 18 arterial segments (for reviewers 1, 2 and 3, respectively), with statistical significance achieved for all three reviewers within the aortic arch, the brachiocephalic artery, as well as bilaterally in the common carotid arteries and in the V1 and V3 segments of the vertebral arteries ($P<0.05$). In comparison with TOF, the left and right proximal internal carotid arteries were rated as having higher image quality with QISS by 3 of 3 and 2 of 3 reviewers, respectively ($P<0.05$).

The image quality of QISS exceeded that of TOF in 7 of 8, 5 of 8, and 8 of 8 carotid arterial segments for reviewers 1, 2, and 3 ($P<0.01$), and in 6 of 8, 6 of 8, and 5 of 8 vertebral artery segments for reviewers 1, 2, and 3 ($P<0.05$).

Image Quality – Inter-rater and Intra-rater Agreement

Inter-rater agreement was moderate for the nonenhanced techniques of QISS (AC1=0.43, 95% CI: 0.40–0.46; $P<0.001$) and TOF (AC1=0.41, 95% CI: 0.38–0.43; $P<0.001$), and substantial for CEMRA (AC1=0.70, 95% CI: 0.67–0.72; $P<0.001$). In the twelve randomly selected patients scored twice to evaluate the intra-rater agreement, mean image quality scores and AC1 agreement values for the first and second image quality assessments for reviewer 1 were 2.6 and 2.6 for QISS (AC1=0.71; $P<0.001$), 2.1 and 1.9 for TOF (AC1=0.54; $P<0.001$), and 3.6 and 3.6 for CEMRA (AC1=0.58; $P<0.001$). Corresponding mean image quality scores and intra-rater agreement values for reviewer 2 were 2.8 and 3.4 for QISS (AC1=0.23; $P<0.001$), 2.3 and 2.6 for TOF (AC1=0.33; $P<0.001$), and 3.8 and 3.9 for CEMRA (AC1=0.87; $P<0.001$). Corresponding first and second session mean image quality scores and intra-rater agreement values for reviewer 3 were 3.0 and 3.0 for QISS (AC1=0.52; $P<0.001$), 2.3 and 2.5 for TOF (AC1=0.56; $P<0.001$), and 3.6 and 3.8 for CEMRA (AC1=0.69; $P<0.001$).

Image Quality – Impact of Gender, Age, Body Mass Index

Image quality was rated significantly better in males than in females for QISS (mean scores of 2.9 versus 2.6, $P<0.05$), but not for TOF (2.2 versus 2.1, $P=0.12$) or CEMRA (3.7 versus 3.5, $P=0.13$). There were significant negative correlations between image quality and age for TOF ($\rho=-0.41$, $P<0.01$) and QISS ($\rho=-0.35$, $P<0.01$), but not for CEMRA ($\rho=0.0033$, $P=0.80$). Image quality was negatively correlated with body mass index for CEMRA ($\rho=-0.37$, $P<0.01$) and TOF ($\rho=-0.39$, $P<0.01$), but not for QISS ($\rho=-0.19$, $P=0.14$).

Grading of Carotid Stenosis

In 60 patients, reviewers 1 and 2 respectively scored 4 of 120 and 2 of 120 proximal internal carotid arteries on CEMRA as non-diagnostic. In the remaining segments in which the CEMRA served as the reference test (116 segments for reviewer 1, 118 segments for reviewer 2) (contingency tables provided in Supporting Information), stenosis grades were in almost perfect agreement between QISS and CEMRA for reviewer 1 (AC1=0.94, 95% CI: 0.89–0.98; P<0.001), and for reviewer 2 (AC1=0.89, 95% CI: 0.83–0.95; $P<0.001$). Stenosis grades demonstrated significantly poorer agreement between TOF and CEMRA for reviewer 1 (AC1=0.73, 95% CI: 0.64–0.83; $P<0.001$) and reviewer 2 (AC1=0.68, 95% CI: 0.58–0.78; $P<0.001$). Inter-rater agreement in stenosis gradings were almost perfect for QISS (AC1=0.95, 95% CI: 0.90–0.99; $P<0.001$) and CEMRA (AC1=0.93, 95% CI: 0.88–0.98; $P<0.001$), and exceeded values provided by 2D TOF (AC1=0.76, 95% CI: 0.67–0.85; $P<0.001$).

After dichotomizing the data, the sensitivity and specificity of QISS for the detection of ≥50% carotid stenosis with respect to CEMRA for reviewer 1 were 57% (4/7, 95% CI: 20–80%) and 100% (90/90, 95% CI: 95–100%), respectively; corresponding values for 2D TOF were 86% (6/7, 95% CI: 42–99%) and 91% (82/90, 95% CI: 83–96%), respectively. For

reviewer 2, the sensitivity and specificity values were 45% (5/11, 95% CI: 18–75%) and 100% (85/85, 95% CI: 95–100%) for QISS, and 27% (3/11, 95% CI: 7–61%) and 93% (79/85, 95% CI: 85%−97%) for TOF.

DISCUSSION

In this retrospective study comparing ungated radial QISS using a FLASH readout, 2D TOF and CEMRA of the carotid bifurcation and other cervical arteries at 3 Tesla, QISS provided significantly better image quality and more diagnostic arterial segments than 2D TOF. Moreover, QISS showed better agreement with CEMRA for grading stenosis of the proximal internal carotid artery.

CEMRA provided the best image quality and inter-rater agreement in displaying neck arteries, which is in line with prior studies (1, 17, 18, 21, 22). Despite its lower accuracy, we routinely acquire 2D TOF prior to CEMRA in order to provide a scout for placement of the 3D slab as well as a backup in case of a technical failure during the contrast-enhanced study. TOF techniques are also used to evaluate patients who cannot receive Gd-based contrast agents, or for situations where the contrast agent is reserved for a subsequent brain perfusion study. We found that QISS provided better image quality than 2D TOF in a large majority (≈70–80%) of neck arterial segments. Moreover, the improvement in image quality for QISS in comparison with 2D TOF significantly increased the fraction of diagnostic arterial segments according to all three radiologist reviewers.

Clinically, the most common arterial pathologies of the neck include stenoses of proximal internal carotid arteries and V1 segments of the vertebral arteries, as well as dissections affecting the proximal and cervical internal carotid arteries and the V2 and V3 segments of the vertebral arteries (23–27). In these arterial locations, (spanning 10 arterial segments scored for image quality), QISS provided significantly better image quality than 2D TOF according to a majority of the three reviewers in 90% (9/10) of cases.

The improved image quality of QISS with respect to 2D TOF is partly ascribed to the fact that the two imaging techniques utilize different mechanisms for background and venous signal suppression. With 2D TOF, a large excitation flip angle (60°) is required to achieve adequate background suppression. With QISS, the use of in-plane inversion allows adequate background suppression with a much lower excitation flip angle (30°), resulting in less saturation of inflowing arterial spins. Another difference is that with TOF, the traveling venous saturation pulse is applied every sequence repetition time of 24ms, whereas with QISS the traveling venous inversion pulse is applied much less often – only once every 1100ms. The combination of the two-fold lower excitation flip angle with the less frequent application of the venous inversion RF pulse reduces the likelihood of inadvertent flow suppression in horizontally-directed or tortuous arterial segments such as in the carotid siphons and V3 segments of the vertebral arteries.

A previous pilot study of QISS for the neck vessels differs from the current study in that it used ECG gating and Cartesian k-space sampling (15). The current study was performed in a busy clinical environment where high patient throughput was essential. We chose to use an

ungated implementation of QISS since our technologists do not routinely apply ECG leads for neurovascular exams, and doing so would increase the time for patient set-up. Second, due to the oversampling of central k-space, radial sampling is less motion-sensitive than Cartesian sampling (28), which helps to minimize artifacts from swallowing, as well as from respiration for the intra-thoracic segments of the carotid and vertebral arteries. Of note, the radial QISS acquisition used this study was roughly 3-fold undersampled with respect to the Nyquist sampling rate (204 versus 603 radial views). Further increases in the undersampling rate may be possible, although signal-to-noise considerations may require modest reductions of the imaging matrix or the use of advanced image reconstruction techniques.

As with QISS MRA of the lower extremities (13), QISS of the neck vessels was designed to be a straightforward technique for the MR technologists. Protocol parameters are fixed, and no patient-specific changes are needed. The large field-of-view and 23.5cm of head-to-foot coverage helps to reduce the likelihood that vessels of interest could be inadvertently excluded from the imaged region. Of the 112 arterial segments that were not fully contained by the QISS field-of-view and thus excluded from analysis, the majority (88%), were from the petrous internal carotid arteries, and V4 and V3 segments of the vertebral arteries. Upon retrospective review of the acquired data, these vessel segments were not located within the QISS volume because the imaging volume was positioned below (median=1.7cm, interquartile range=0.6–3.1cm) the carotid bifurcation, and not at level of the carotid bifurcation as is optimal from our experience. Acquisition of a several additional imaging slices or use of less slice overlap would extend coverage to easily address this limitation.

The standard QISS technique used for peripheral artery MRA was modified in several key respects to adapt it for imaging of the head and neck vessels. First, a radial k-space trajectory was used instead of the usual Cartesian trajectory to minimize motion artifacts from swallowing and respiration, while a FLASH readout was used instead of the usual bSSFP readout to avoid off-resonance artifacts. Second, slices were tilted 45° towards a coronal orientation, providing more efficient head-to-foot spatial coverage and reducing scan time by a factor of $\sqrt{2}$ compared with the axial slices used for peripheral MRA. Third, no ECG gating was used. Whereas blood flow in healthy peripheral arteries is triphasic, including periods of stasis and reverse flow, arterial blood flow in the neck is continuous. While ECG gating is critical for optimal image quality in triphasic lower extremities arteries, we have found it to be superfluous for the monophasic head and neck vessels.

In contrast to previously-described volumetric nonenhanced MRA techniques (9, 11, 12), QISS uses a slice-selective acquisition that requires only a few millimeters of arterial inflow for complete refreshment of saturated in-plane spins. Consequently, we anticipate that the technique should be effective even in the setting of very slow flow. The QISS technique proved more resistant than TOF to motion artifacts in the upper thorax for imaging of the carotid and vertebral origins. Finally, it should be noted that the QISS protocol was set up to span a region from approximately the aortic arch through the skull base in 7 minutes. In cases where the clinical concern is focused on the carotid bifurcation, the number of slices can be greatly reduced, and the scan time decreased to a few minutes or less.

Image quality for QISS was rated better in males than in females. We speculate that this may be due to gender differences in arterial size or blood flow velocity. As with 2D TOF, there was a negative relationship between image quality and age. This could be due to increased arterial tortuosity and reduced blood flow velocities found in older patients, or the tendency for older patients to move more frequently or breathe more deeply during the exams. Finally, unlike 2D TOF and CEMRA, there was no significant negative association of image quality with body mass index with QISS. This may relate to the use of an in-plane inversion pulse with QISS which suppresses the signal from stationary background tissues. Of note, no chemically selective fat signal suppression was used with QISS as it can inadvertently saturate off-resonant arterial signal located at the edges of the scanner bore.

This study had some potential limitations. First, we did not compare ungated radial QISS to 3D TOF, which can provide higher spatial resolution than 2D TOF at the carotid bifurcation (7, 29). 3D TOF is not routinely acquired at our institution due to its motion sensitivity, tendency towards saturation artifacts in the setting of tortuous vessels or slow flow, and limited spatial coverage. Second, because of the retrospective nature of the study, the scans were not acquired in a random order – 2D TOF was acquired first, followed by QISS and CEMRA. Third, some arterial segments, such as the petrous ICA and V4 segments of the vertebral arteries, were often rated as fair with QISS; further technical improvements or better volume positioning to better display these segments would be desirable. Fourth, inter-rater and intra-rater agreements of subjective image quality scores were lower for QISS than for CEMRA, suggesting that there is a need for further optimization of the non-contrast technique. Nonetheless, inter-rater agreement and methodological agreement (QISS versus CEMRA) for carotid stenosis gradings were almost perfect (AC1≈0.89 or greater) in our study. Finally, our patient cohort was relatively small and involved a single institution. Evaluation of the diagnostic performance of QISS versus TOF will require a prospective multi-center trial involving more patients with arterial pathology.

In conclusion, QISS provided significantly better image quality and more diagnostic arterial segments overall than standard-of-care 2D TOF, and demonstrated improved agreement with CEMRA for grading stenosis of the proximal internal carotid artery. Given its superior performance, ungated radial QISS has the potential to replace 2D TOF for the nonenhanced evaluation of the neck arteries. Based on these promising initial results, further clinical validation appears warranted.

Supplementary Material

Refer to Web version on PubMed Central for supplementary material.

Acknowledgments:

The authors wish to thank Ms. Claire Feczko and Dr. Ali Serhal for their assistance with this study. This work was supported in part by the National Institute of Biomedical Imaging and Bioengineering of the National Institutes of Health under award number R01EB027475. The content is solely the responsibility of the authors and does not necessarily represent the official views of the National Institutes of Health.

REFERENCES

1. Phan T, Huston J 3rd, Bernstein MA, Riederer SJ, Brown RD Jr.. Contrast-enhanced magnetic resonance angiography of the cervical vessels: experience with 422 patients. Stroke 2001; 32:2282–2286. [PubMed: 11588314]
2. Wright VL, Olan W, Dick B, et al. Assessment of CE-MRA for the rapid detection of supra-aortic vascular disease. Neurology 2005; 65:27–32. [PubMed: 16009882]
3. Debrey SM, Yu H, Lynch JK, et al. Diagnostic accuracy of magnetic resonance angiography for internal carotid artery disease: a systematic review and meta-analysis. Stroke 2008; 39:2237–2248. [PubMed: 18556586]
4. Latchaw RE, Alberts MJ, Lev MH, et al. Recommendations for imaging of acute ischemic stroke: a scientific statement from the American Heart Association. Stroke 2009; 40:3646–3678. [PubMed: 19797189]
5. Boujan T, Neuberger U, Pfaff J, et al. Value of Contrast-Enhanced MRA versus Time-of-Flight MRA in Acute Ischemic Stroke MRI. AJNR Am J Neuroradiol 2018; 39:1710–1716. [PubMed: 30115678]
6. Huston J 3rd, Lewis BD, Wiebers DO, Meyer FB, Riederer SJ, Weaver AL. Carotid artery: prospective blinded comparison of two-dimensional time-of-flight MR angiography with conventional angiography and duplex US. Radiology 1993; 186:339–344. [PubMed: 8421731]
7. De Marco JK, Nesbit GM, Wesbey GE, Richardson D. Prospective evaluation of extracranial carotid stenosis: MR angiography with maximum-intensity projections and multiplanar reformation compared with conventional angiography. AJR Am J Roentgenol 1994; 163:1205–1212. [PubMed: 7976902]
8. Yucel EK, Anderson CM, Edelman RR, et al. AHA scientific statement. Magnetic resonance angiography : update on applications for extracranial arteries. Circulation 1999; 100:2284–2301. [PubMed: 10578005]
9. Kramer H, Runge VM, Morelli JN, et al. Magnetic resonance angiography of the carotid arteries: comparison of unenhanced and contrast enhanced techniques. Eur Radiol 2011; 21:1667–1676. [PubMed: 21476128]
10. Takei N, Miyoshi M, Kabasawa H. Noncontrast MR angiography for supraaortic arteries using inflow enhanced inversion recovery fast spin echo imaging. J Magn Reson Imaging 2012; 35:957–962. [PubMed: 22127993]
11. Raoult H, Gauvrit JY, Schmitt P, Le Couls V, Bannier E. Non-ECG-gated unenhanced MRA of the carotids: optimization and clinical feasibility. Eur Radiol 2013; 23:3020–3028. [PubMed: 23783783]
12. Koktzoglou I, Walker MT, Meyer JR, Murphy IG, Edelman RR. Nonenhanced hybridized arterial spin labeled magnetic resonance angiography of the extracranial carotid arteries using a fast low angle shot readout at 3 Tesla. J Cardiovasc Magn Reson 2016; 18:18. [PubMed: 27067840]
13. Edelman RR, Sheehan JJ, Dunkle E, Schindler N, Carr J, Koktzoglou I. Quiescent-interval single-shot unenhanced magnetic resonance angiography of peripheral vascular disease: Technical considerations and clinical feasibility. Magn Reson Med 2010; 63:951–958. [PubMed: 20373396]
14. Hodnett PA, Koktzoglou I, Davarpanah AH, et al. Evaluation of peripheral arterial disease with nonenhanced quiescent-interval single-shot MR angiography. Radiology 2011; 260:282–293. [PubMed: 21502384]
15. Koktzoglou I, Murphy IG, Giri S, Edelman RR. Quiescent interval low angle shot magnetic resonance angiography of the extracranial carotid arteries. Magn Reson Med 2016; 75:2072–2077. [PubMed: 26072706]
16. Koktzoglou I, Edelman RR. Super-resolution intracranial quiescent interval slice-selective magnetic resonance angiography. Magn Reson Med 2018; 79:683–691. [PubMed: 28470792]
17. Willinek WA, von Falkenhausen M, Born M, et al. Noninvasive detection of steno-occlusive disease of the supra-aortic arteries with three-dimensional contrast-enhanced magnetic resonance angiography: a prospective, intra-individual comparative analysis with digital subtraction angiography. Stroke 2005; 36:38–43. [PubMed: 15569881]

18. Nael K, Villablanca JP, Pope WB, McNamara TO, Laub G, Finn JP. Supraaortic arteries: contrast-enhanced MR angiography at 3.0 T--highly accelerated parallel acquisition for improved spatial resolution over an extended field of view. Radiology 2007; 242:600–609. [PubMed: 17255428]
19. Gwet KL. Computing inter-rater reliability and its variance in the presence of high agreement. Br J Math Stat Psychol 2008; 61(Pt 1):29–48. [PubMed: 18482474]
20. Landis JR, Koch GG. The measurement of observer agreement for categorical data. Biometrics 1977; 33:159–174. [PubMed: 843571]
21. Carr JC, Ma J, Desphande V, Pereles S, Laub G, Finn JP. High-resolution breath-hold contrast-enhanced MR angiography of the entire carotid circulation. AJR Am J Roentgenol 2002; 178:543–549. [PubMed: 11856670]
22. Menke J Diagnostic accuracy of contrast-enhanced MR angiography in severe carotid stenosis: meta-analysis with metaregression of different techniques. Eur Radiol 2009; 19:2204–2216. [PubMed: 19399505]
23. Fisher CM, Gore I, Okabe N, White PD. Atherosclerosis of the carotid and vertebral arteries—extracranial and intracranial. J Neuropathol Exp Neurol 1965; 24:455–476.
24. Rodallec MH, Marteau V, Gerber S, Desmottes L, Zins M. Craniocervical Arterial Dissection: Spectrum of Imaging Findings and Differential Diagnosis. RadioGraphics 2008; 28:1711–1728. [PubMed: 18936031]
25. Mazighi M, Labreuche J, Gongora-Rivera F, Duyckaerts C, Hauw J-J, Amarenco P. Autopsy Prevalence of Proximal Extracranial Atherosclerosis in Patients With Fatal Stroke. Stroke 2009; 40:713–718. [PubMed: 19118247]
26. Arnold M, Bousser MG, Fahrni G, et al. Vertebral Artery Dissection. Stroke 2006; 37:2499–2503. [PubMed: 16960096]
27. Schievink WI. Spontaneous Dissection of the Carotid and Vertebral Arteries. N Engl J Med 2002; 344:898–906.
28. Glover GH, Pauly JM. Projection reconstruction techniques for reduction of motion effects in MRI. Magn Reson Med 1992; 28:275–289. [PubMed: 1461126]
29. Scarabino T, Carriero A, Magarelli N, et al. MR angiography in carotid stenosis: a comparison of three techniques. Eur J Radiol 1998; 28:117–125. [PubMed: 9788013]

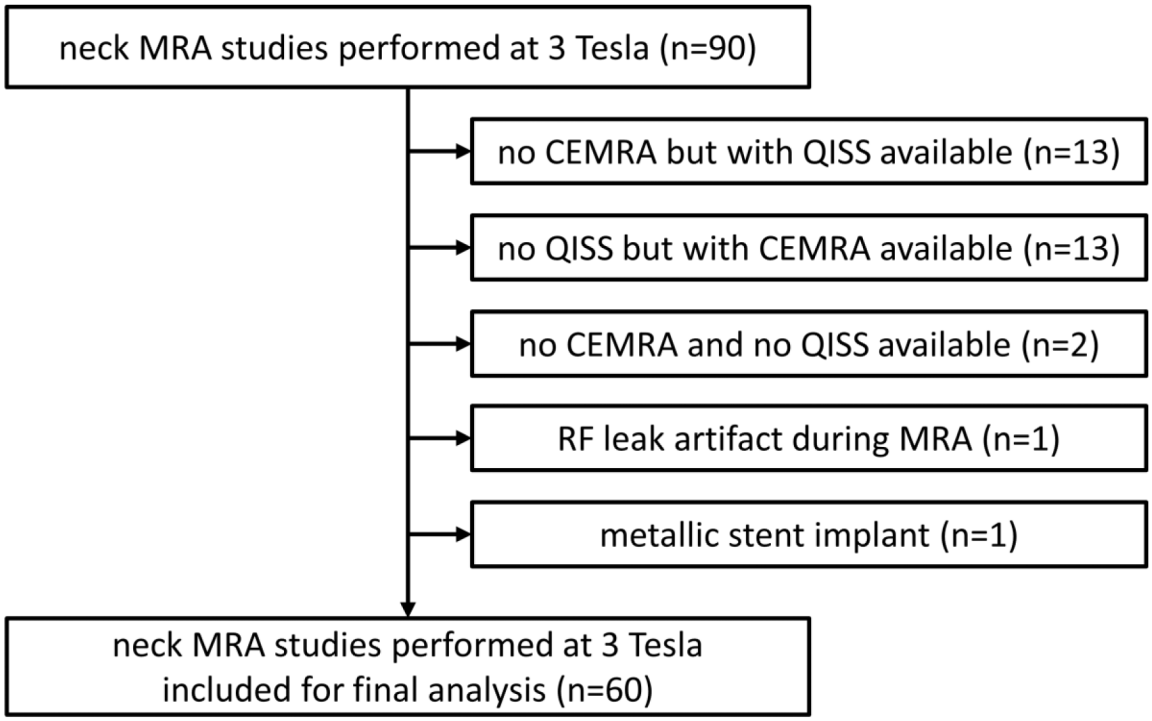

Figure 1.

Flow chart diagram shows patient inclusion process for the study. MRA = magnetic resonance angiography. CEMRA = contrast-enhanced magnetic resonance angiography. QISS = quiescent interval slice-selective. RF = radiofrequency.

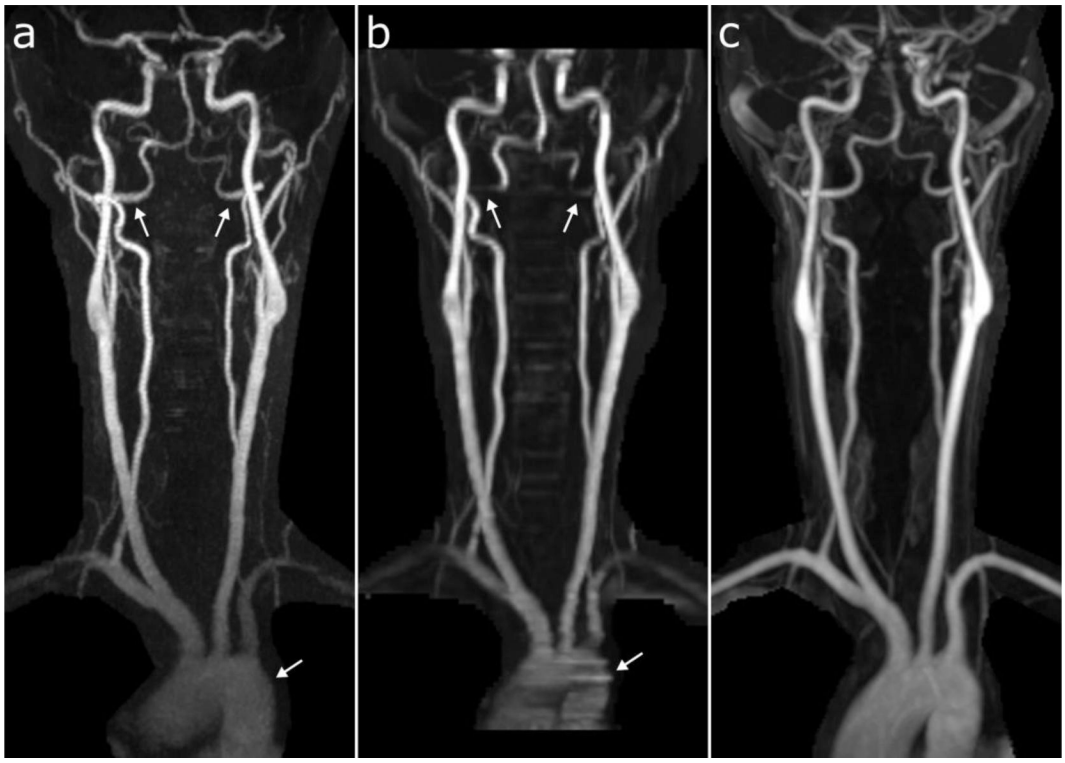

Figure 2.

Representative coronal maximum intensity projection images obtained with **(a)** ungated radial QISS, **(b)** TOF, and **(c)** CEMRA. Note the superior image quality of ungated radial QISS with respect to TOF, especially noticeable in the aortic arch and V3 segments of the vertebral arteries (arrows). All 18 of 18 arterial segments were deemed scorable in this patient by all three imaging techniques and reviewers. The percentages of these 18 segments with diagnostic image quality were: 100% (18/18) for QISS and CEMRA (all reviewers); and 77.8% (14/18), 94.4% (17/18), and 88.9% (16/18) for TOF (reviewers 1, 2, and 3, respectively).

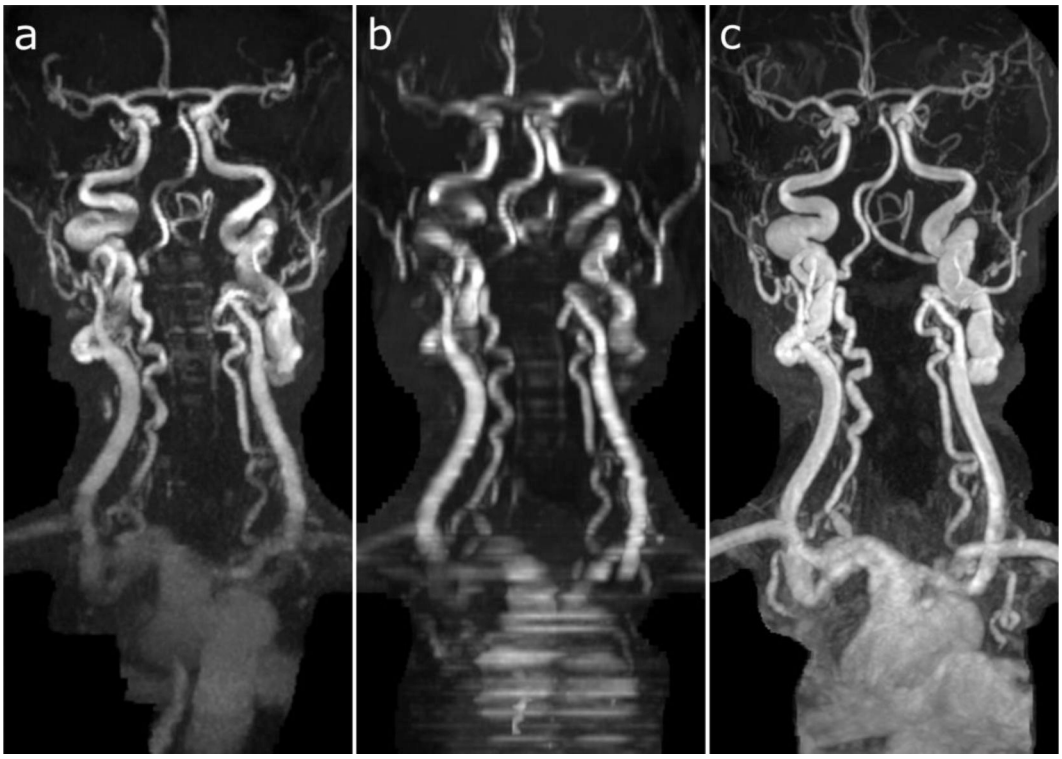

Figure 3.

Coronal maximum intensity projection images obtained with **(a)** ungated radial QISS, **(b)** TOF, and **(c)** CEMRA in a patient with arterial ectasia of the carotid and vertebral arteries. While there is some in-plane flow saturation apparent on both nonenhanced ungated radial QISS and TOF protocols due to arterial ectasia, QISS shows much less degradation from motion artifact and in-plane flow saturation. All 18 of 18 arterial segments were deemed scorable in this patient by all three imaging techniques and reviewers. The percentages of these 18 segments with diagnostic image quality were: 77.8% (14/18), 55.6% (10/18), and 77.8% (14/18) for QISS (reviewers 1, 2, and 3, respectively); 33.3% (6/18), 11.1% (2/18), and 38.9% (7/18) for TOF (reviewers 1, 2, and 3, respectively); and 100% (18/18) for CEMRA (all reviewers).

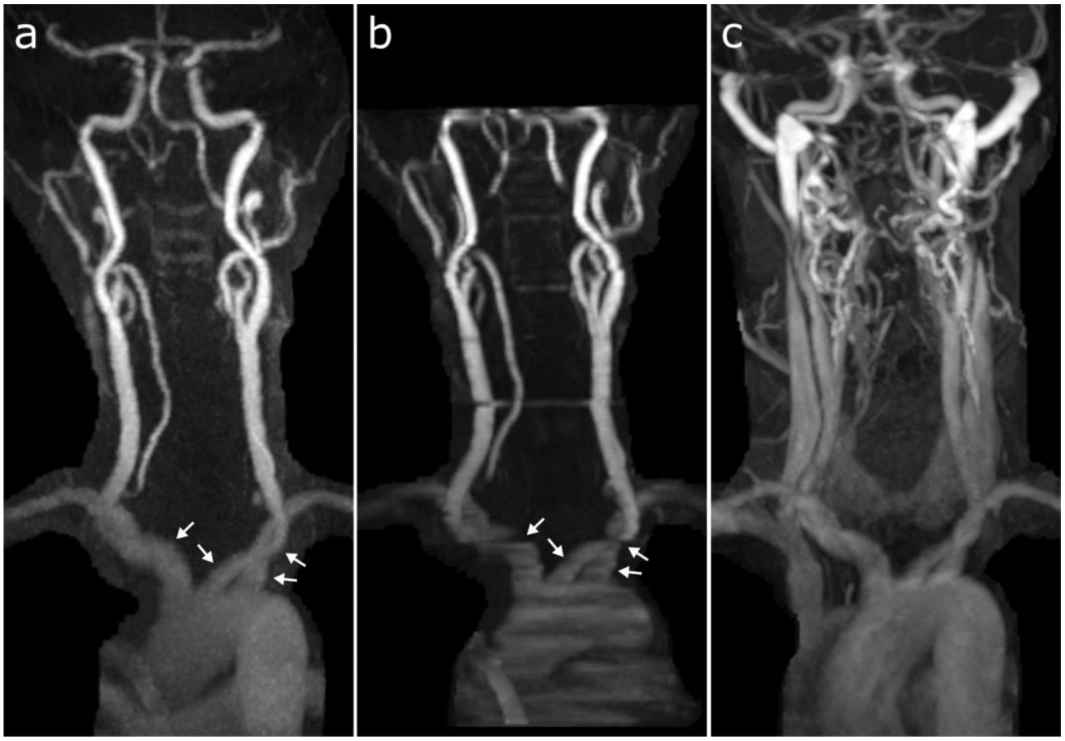

Figure 4.

Coronal maximum intensity projection images obtained with **(a)** ungated radial QISS, **(b)** TOF, and **(c)** CEMRA in a patient where there was substantial venous contamination during CEMRA from a late acquisition with respect to the time of contrast bolus arrival. Compared with TOF, QISS better depicts the proximal carotid, subclavian, and brachiocephalic arteries (arrows) and shows less motion artifact in the common carotid artery. Sixteen of 18 arterial segments were deemed scorable in this patient by all three imaging techniques and reviewers. The percentages of these 16 segments with diagnostic image quality were: 100% (16/16) for QISS (all reviewers); 62.5% (10/16), 68.8% (11/16), and 93.8% (15/16) for TOF (reviewers 1, 2, and 3, respectively); and 37.5% (6/16), 56.3% (9/16), and 56.3% (9/16) for CEMRA (reviewers 1, 2, and 3, respectively).

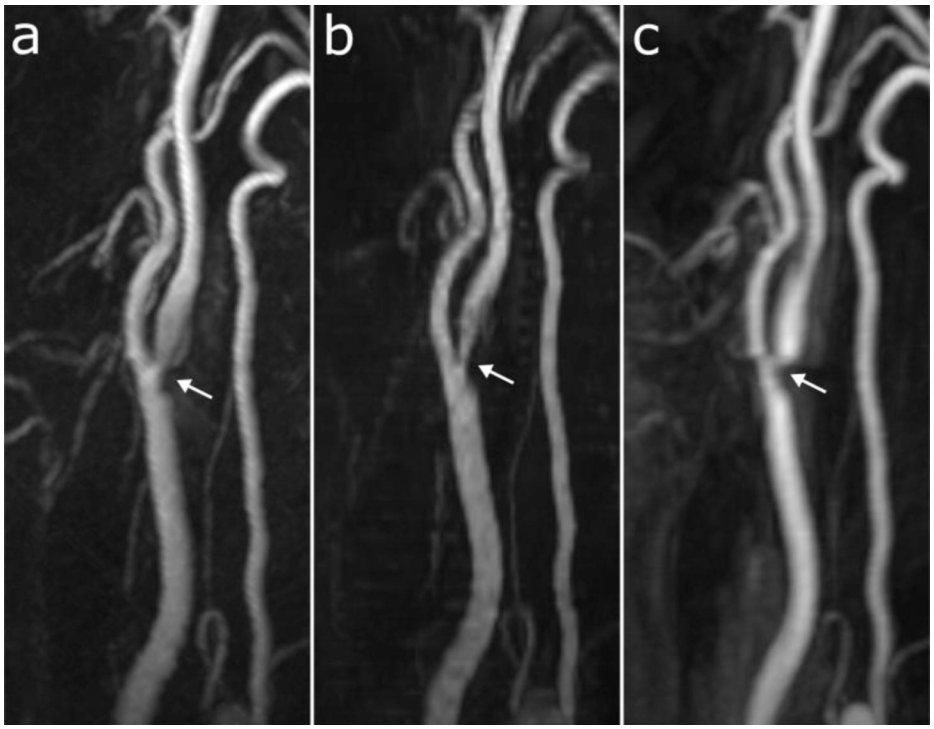

Figure 5.

Patient with moderate stenosis (arrows) at the right carotid bifurcation. Sagittal 60mm-thick maximum intensity projection images obtained with **(a)** ungated radial QISS, **(b)** TOF, and **(c)** CEMRA. Note that the severity and extent of the stenosis is exaggerated by TOF, whereas there is good correspondence between QISS and CEMRA.

Table 1.

Imaging Parameters[a]

	QISS[b]	TOF	CEMRA
Slice orientation	oblique axial[c]	axial	coronal
Acquisition type	2D radial	2D Cartesian	3D Cartesian
TR / TE (ms)	15.0 / 4.9	24.0 / 4.6	3.2 / 1.2
Sequence TR (ms)	1100	24.0	3.2
Flip angle (degrees)	30	60	25
Field of view (mm)	416 × 416	210 × 210	340 × 298
Matrix	384 × 384	256 × 256	384 × 276
Acquired in-plane resolution (mm)	1.08 × 1.08	0.82 × 0.82	0.89 × 1.08
Slices acquired[d]	128	125	60 (96)
Slice thickness (mm)[d]	2.0	3.0	1.8 (1.1)
Slice overlap (mm)	0.7	1.0	--
Axial coverage (mm)	235[e]	256	340
Phase / Slice partial Fourier	--	off / off	$6/8^{th}$ / $6/8^{th}$
Slice oversampling	--	--	8.3%
Parallel imaging factor	--	--	3
Flow compensation	yes	yes	no
Bandwidth (Hz/pixel)	500	219	590
Scan time (s)	414	421	16

[a] Values are medians across 60 acquisitions.

[b] QISS used 3 imaging shots (i.e. sequence TRs) per slice, and collected a total of 204 radial views (i.e. 68 radial views per imaging shot).

[c] 45° slice tilt between axial and coronal planes.

[d] Values for CEMRA provided as: acquired (reconstructed after interpolation).

[e] Includes √2-fold increased coverage from tilted slice acquisition.

Table 2.

Percentage of Diagnostic Arterial Segments

				P-Value, QISS vs.	
	QISS	**TOF**	**CEMRA**	**TOF**	**CEMRA**
Reviewer 1	91.0% (88.9, 92.7)	71.7% (68.6, 74.5)	97.1% (95.7, 98.0)	<0.0001	<0.0001
Reviewer 2	93.5% (91.6, 95.0)	72.9% (69.9, 75.8)	97.4% (96.0, 98.3)	<0.0001	<0.001
Reviewer 3	95.5% (93.9, 96.7)	85.2% (82.7, 87.5)	96.8% (95.4, 97.8)	<0.0001	0.18

Data presented as: percentage (95% confidence interval). Percentages derived from the 908 arterial segments included in final analysis.

Table 3.

Image Quality Scores

Segments	Reviewer 1#			Reviewer 2#			Reviewer 3#		
	QISS	TOF	CEMRA	QISS	TOF	CEMRA	QISS	TOF	CEMRA
1. Aortic Arch	2.7[a]	1.4	3.3[b]	2.8[a]	1.4	3.6[b]	2.8[a]	1.8	3.4[b]
2. Brachiocephalic Artery	2.7[a]	1.7	3.2[b]	2.8[a]	1.5	3.6[b]	2.8[a]	1.8	3.4[b]
3. Left CCA	2.5[a]	1.6	3.3[b]	2.8[a]	1.8	3.7[b]	3.2[a]	2.2	3.6[b]
4. Right CCA	2.6[a]	1.9	3.4[b]	2.8[a]	1.9	3.7[b]	3.2[a]	2.2	3.7[b]
5. Left Proximal ICA	2.9[a]	2.4	3.8[b]	2.8[a]	2.6	3.7[b]	3.4[a]	2.7	3.7[b]
6. Right Proximal ICA	2.8[a]	2.4	3.8[b]	2.8	2.6	3.7[b]	3.4[a]	2.7	3.7[b]
7. Left Cervical ICA	2.7[a]	2.4	3.8[b]	2.7	2.6	3.8[b]	3.2[a]	2.7	3.7[b]
8. Right Cervical ICA	2.8[a]	2.5	3.8[b]	2.7	2.6	3.8[b]	3.3[a]	2.8	3.7[b]
9. Left Petrous ICA	2.5[a]	1.9	3.6[b]	2.2[a]	1.8	3.9[b]	2.4[a]	1.9	3.8[b]
10. Right Petrous ICA	2.3	2.0	3.6[b]	2.3[a]	1.8	3.9[b]	2.8[a]	2.1	3.8[b]
11. Left Vertebral – V1	2.4[a]	2.0	3.6[b]	2.8[a]	2.2	3.7[b]	2.8[a]	2.3	3.2[b]
12. Right Vertebral – V1	2.6[a]	2.1	3.5[b]	2.9[a]	2.3	3.7[b]	2.7[a]	2.4	3.1[b]
13. Left Vertebral – V2	2.9[a]	2.7	3.7[b]	2.9	3.0	3.7[b]	3.2[a]	3.0	3.6[b]
14. Right Vertebral – V2	2.9[a]	2.7	3.6[b]	2.8	2.9	3.7[b]	3.1	3.0	3.6[b]
15. Left Vertebral – V3	2.7[a]	1.4	3.7[b]	2.7[a]	2.1	3.7[b]	2.8 [a]	1.8	3.5[b]
16. Right Vertebral – V3	2.6[a]	1.4	3.7[b]	2.7[a]	2.0	3.6[b]	2.7[a]	1.8	3.5[b]
17. Left Vertebral – V4	2.5	2.2	3.8[b]	2.1[a]	1.6	3.7[b]	2.1	1.9	3.5[b]
18. Right Vertebral – V4	2.2	2.0	3.7[b]	2.1[a]	1.5	3.7[b]	2.0	1.8	3.4[b]
All Segments	2.7[a]	2.0	3.6[b]	2.7[a]	2.2	3.7[b]	2.9[a]	2.3	3.5[b]

Data are presented as means; 1: non-diagnostic, 2: fair, 3: good; 4: excellent.

CCA=common carotid artery. ICA=internal carotid artery.

[#] $P<0.05$, Bonferroni-corrected Friedman test across three techniques for all segments.

[a] $P<0.05$, post-hoc Wilcoxon signed-rank test versus TOF for same reviewer.

[b] $P<0.05$, post-hoc Wilcoxon signed-rank tests versus QISS and TOF for same reviewer.